# Trivalent Atom Contribution on Solid−Solid Transformation of $Ga_{13}$ Polycation Intercalated Clay into Sodalite Investigated by X-ray Absorption Spectroscopy

**Sung-Reol Lee,[†] Man Park,[‡] Yang-Su Han,[‡] Sung-Ho Hwang,[‡] and Jin-Ho Choy*,[†]**

*Division of Nano Science and Department of Chemistry, Ewha Womans University, Seoul 120-750, Korea, and School of Chemistry and Molecular Engineering, Seoul National University, Seoul 151-747, Korea*

*Received: January 3, 2005; In Final Form: March 4, 2005*

Solid−solid transformation mechanism of Ga Keggin-type ion intercalated clay into sodalite has been clarified by X-ray diffraction (XRD), FT-IR spectroscopy, and X-rayabsorption spectroscopy (XAS). To follow the structural evolution precisely by XANES and EXAFS, the XAS active element containing polycation $[Ga_{13}O_4(OH)_{24}(H_2O)_{12}]^{7+}$ was intercalated into montmorillonite (MMT). FT-IR and XAS spectra confirm that the formation of sodalite framework is initiated by the delocalized rearrangement between silicate networks and collapsed interlayered Ga species, and is followed by the incorporation of Al in the octahedral sheet of clay (MMT). According to the XAS studies, it is found that the formation of Ga(Al)−O−Si species is strongly influenced by the trivalent cations, which are rapidly changed in the environment, followed by reaction with the silicate network of clay during the solid−solid transformation.

## Introduction

Non-hydrothermal syntheses of zeolite have attracted much attention due to some advantages in terms of high production yield and environmentally benign and easy scale-up processes. Particularly, recent interests have arisen from the potential application of massive recycling of aluminosilicate wastes and preparation of discrete nanocrystalline zeolites.[1−3] However, the detailed reaction mechanism of the solid−solid transformation has not been well-established yet due to the shortage of molecular-level information on the change in chemical environment around framework elements during the crystallization reaction.[4] Recently, we reported unprecedented evidence on the solid−solid transformation of pillared clay into sodalite using X-ray diffraction (XRD), Fourier transform infrared (FT-IR) spectroscopy, $^{27}Al$ and $^{29}Si$ magic angle spinning (MAS) NMR spectroscopy, scanning electron microscopy (SEM), and high-resolution transmission electron microscopy (HR-TEM).[5] Nevertheless, the molecular-level elucidation of the transformation mechanism is still not accomplished. Therefore, we have turned to X-ray absorption spectroscopy (XAS) to elucidate the evolution of framework from elemental components such as Si and Al during the solid−solid transformation process. Although the low-energy X-absorption fine structure setup has been developed, it is still difficult to identify the local structural information on the neighboring atoms by XAS analyses of Si and Al.[6] Herein, we have modified the aluminosilicate system with heavy atoms such as Ga instead of Al because of its high X-ray absorption property. Since Ga has chemical properties similar to those of Al, the gallosilicate derivatives isostructural to aluminosilicate compounds could be readily synthesized by isomorphous substitution of Ga for Al in the framework.[7]

XAS is an element-specific technique that provides detailed information about the local atomic structure.[8] From X-ray absorption near edge structure (XANES) analysis, one can extract the information on electronic structure, oxidation state and coordination number of a specific element. On the other hand, the extended X-ray absorption fine structure (EXAFS) is sensitive to the local environment around the specific atoms that absorb X-rays, which gives the information on the type and number of nearest-neighboring atoms around the X-ray absorbing atoms and the average interatomic distances through the radial distribution function.

In this study, we have prepared the single phasic gallosilicate sodalite from clay (MMT) intercalated with $Ga_{13}$ Keggin type polycation, as previously reported.[5] To elucidate the evolution of framework during the solid−solid transformation process, the transformation of $Ga_{13}$ polycation intercalated clay to the sodalite has been carefully monitored at the molecular level as a function of the reaction time by XANES and EXAFS analyses.

## Experimental Section

The $Ga_{13}$-intercalated clay (GIC) was prepared by conventional ion exchange reaction between the interlayer $Na^+$ ions in montmorillonite (Kunipia F, $((Na_{0.35}K_{0.01}Ca_{0.02})(Si_{3.89}Al_{0.11})(Al_{1.60}Mg_{0.32}\ Fe_{0.08})O_{10}(OH)_2 \cdot nH_2O$, cation exchange capacity = 100 eq/kg) and $Ga_{13}$ polycation ($[Ga_{13}O_4(OH)_{24}(H_2O)_{12}]^{7+}$, Keggin-type ions).[9] The GIC gel prepared by addition of 25 wt % water was well mixed with powdered NaOH at a typical mole ratio of $[OH^-]/[Si] = 10$, and then the resulting gel mixture was thermally treated at 80 °C under an ambient atmosphere. To investigate the transformation process under isothermal conditions, a part of the reaction product was removed periodically from the reaction mixture and used for subsequent analyses. The products obtained at various reaction stages were washed, dried, and analyzed.

Powder XRD patterns were obtained with a Philips PW1830 automated powder X-ray diffractometer with Cu−Kα radiation ($\lambda = 1.5418$ Å). FT-IR spectra were recorded on a Bruker IFS-88 FT-IR spectrometer using the standard KBr disk method. Spectra were acquired at 2 $cm^{-1}$ resolutions and averaged by

* Corresponding author. Fax +82-2-3277-4340; Tel +82-2-3277-4135; E-mail jhchoy@ewha.ac.kr

[†] Ewha Womans University.

[‡] Seoul National University.

10.1021/jp050011k CCC: $30.25 
Published on Web 04/16/2005

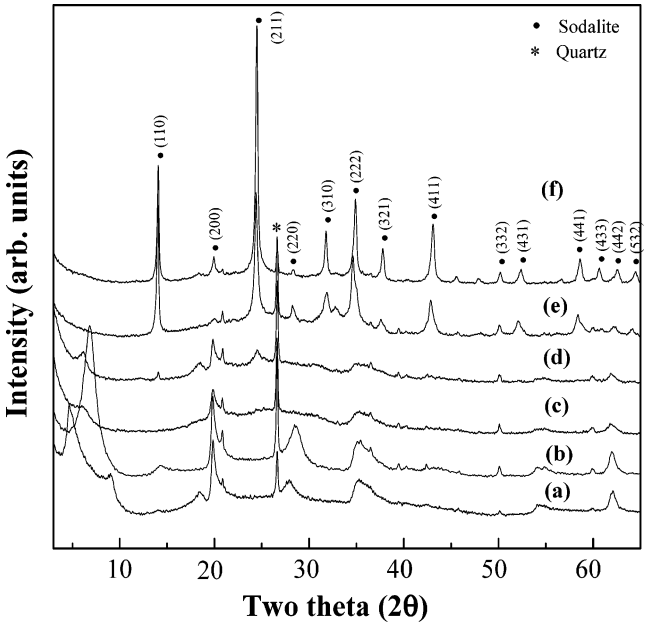


**Figure 1.** Powder X-ray diffraction patterns of (a) GIC and the reaction products obtained by the solid−solid transformation at 80 C as a function of the reaction times, (b) after preparing the solid gel mixture of GIC and NaOH, (c) 30 min, (d) 80 min, (e) 110 min, and (f) 240 min.

64 scans. Elemental analyses of the reaction products were carried out by atomic absorption spectroscopy (ANALAB-9100). For the samples, the reaction products were fused with lithium metaborate ($LiBO_2$) at 900 °C for 10 min and subsequently dissolved in a 10% nitric acid solution.

The X-ray absorption measurements at the Ga K-edge were carried out with synchrotron radiation using EXAFS facilities installed at beam line 10B in the Photon Factory, Tsukuba, which was operated with a ring energy of 2.5 GeV and a stored current of 269 ∼ 370 mA. The spectra were recorded in transmission mode at room temperature with a Si (311) channel-cut monochromator ($d$ = 1.6375 Å). The estimated resolution was about 1 eV at the Ga K-edge (10371 eV). All the data were recorded with a spacing of ∼0.5 eV for the XANES region and 1 eV for the EXAFS region. The data analysis for the experimental spectra was carried out by the standard procedure as reported previously.[6]

## Results and Discussion

**Conventional Characterizations.** Figure 1 represents the XRD patterns of GIC and the reaction products prepared at 80 °C under an ambient atmosphere as a function of reaction period. The GIC shows the interlayer distance of 19.01 Å to reveal the incorporation of $Ga_{13}$ polycations into the interlayer space of clay. The basal spacing of the GIC is determined to be higher than that of $Al_{13}$ intercalated clay since the $Ga_{13}$ polycation is larger in size than the $Al_{13}$ polycation.[9,10] On preparing the solid gel mixture of GIC and NaOH, the decrease in basal spacing of the GIC indicates the collapse of $Ga_{13}$ polycations in the interlayer space of clay. After heat treatment at 80 °C for 80 min, the sodalite phase appears. As the reaction proceeds, the sodalite phase becomes dominant at the expense of the pristine clay. The resultant sodalite particles show spherical morphology with lamellar character (Figure 2), which also supports the solid−solid transformation of GIC into sodalite without any noticeable perturbation of the pristine layered structure. When the Si/Al(Ga) ratio of the resultant sodalite reaches to about 1,

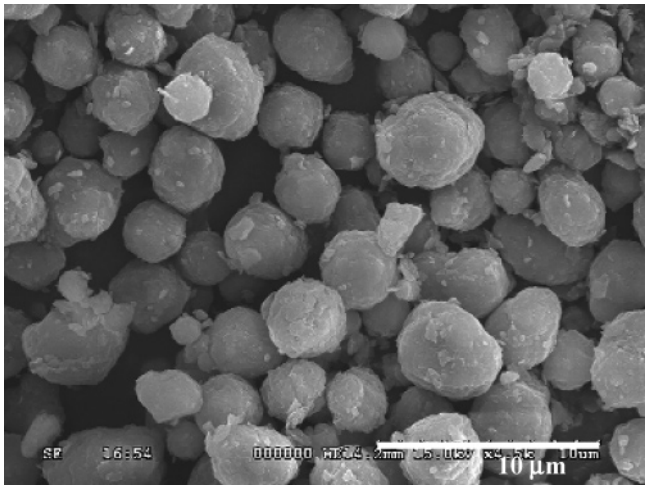


**Figure 2.** Scanning electron micrographs of galliosilicate sodalite.

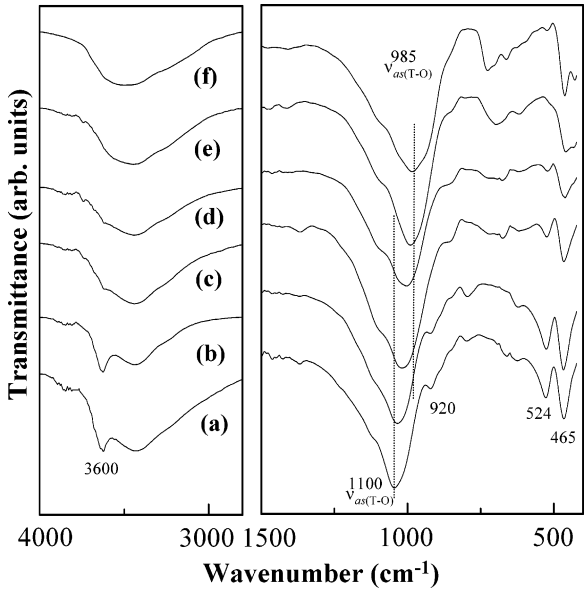


**Figure 3.** FT-IR spectra of (a) GIC and the reaction products obtained by the solid−solid transformation at 80 °C as the function of the reaction times, (b) after preparing the solid gel mixture of GIC and NaOH, (c) 30 min, (d) 80 min, (e) 110 min, and (f) 240 min.

the unit cell parameter ($a_o$ = 8.95 Å) becomes lager than that of sodalite ($a_o$ = 8.92 Å) synthesized from the $Al_2O_3$ pillared clay,[5] which is due to the incorporation of Ga into the sodalite framework. In addition, it is worth noting here that the crystallization of sodalite and the degradation of clay occur simultaneously, without undergoing any X-ray amorphous phases. This result is consistent with our previous result that only a short-range molecular rearrangement occurs in the process of the transformation of $Al_2O_3$ pillared clay into sodalite.[5]

Figure 3 shows the variation of the FT-IR spectra during the solid−solid transformation at 80 C. The vibrational frequencies of the GIC are similar to that of $Al_{13}$-intercalated clay.[5,11] As the reaction proceeds, the gradual peak shift of the Si−O stretching from 1100 to 986 cm$^{-1}$ is observed along with a weakening of the characteristic absorption bands of clay (MMT) at 3630, 920, and 524 cm$^{-1}$. This is evidence that the Ga(Al) atoms are gradually incorporated into tetrahedral $SiO_4$ network to form the zeolitic framework.[12] The diagnostic features of sodalite formation can also be seen as new absorption bands related to the structure-sensitive single four-ring (S4R) of sodalite units at 430 cm$^{-1}$ and the symmetric stretching

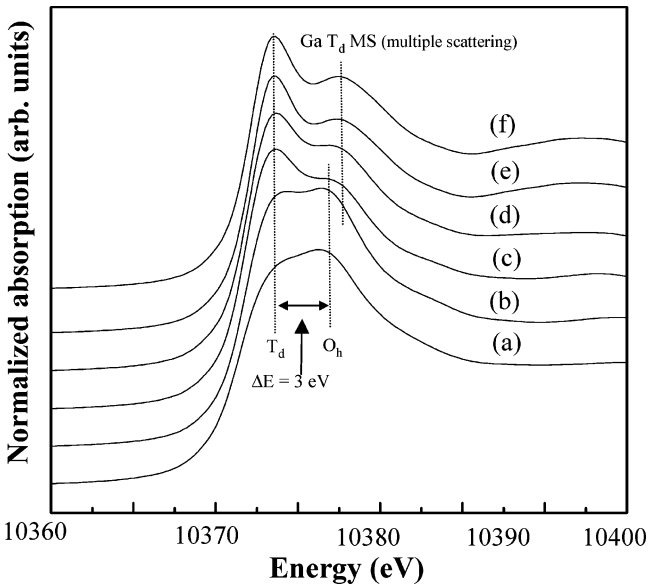


**Figure 4.** Ga K-edge XANES spectra of FT-IR spectra of (a) GIC and the reaction products obtained by the solid−solid transformation at 80 °C as the function of the reaction times, (b) after preparing the solid gel mixture of GIC and NaOH, (c) 30 min, (d) 80 min, and (e) 240 min.

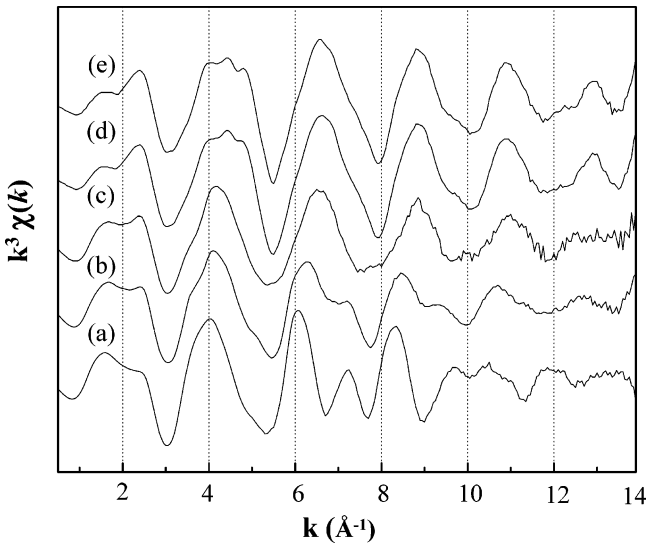


**Figure 5.** $k^3$-Weighted Ga K-edge EXAFS spectra for (a) GIC, (b) after preparing the solid gel mixture of GIC and NaOH and the solid−solid transformation reaction for (c) 30 min, (d) 80 min, and (e) 240 min.

vibrations ($\nu_s$(T−O)) in the 670∼730 cm$^{-1}$ region.[13] These bands become progressively enhanced along with the gradual shift of the Si−O stretching band. On the other hand, the absorption band at 524 cm$^{-1}$, the bending vibration of Si−O−Al (octahedral Al) in clay (MMT),[11] is gradually reduced with the reaction time, indicating that the GIC is transformed into sodalite by topographical rearrangement without any noticeable dissolution, as reported in the transformation of $Al_2O_3$ pillared clay into sodalite.[5]

**Ga K-Edge XANES.** According to the Ga K-edge XANES spectra for the reaction products derived from GICs (Figure 4), it becomes clear that the octahedrally coordinated Ga atoms with oxygen ligands in the GIC change into the tetrahedral atoms in sodalite during solid−solid transformation, which can be rationalized by the lower energy shift of the Ga K-edge due to the electronegativity reduction of the nearest-neighbor ligands.[14] For the GIC (a), the XANES spectrum exhibits two absorption peaks resulting from the $Ga_{13}$ polycation structure with twelve gallium octahedra surrounding a central gallium tetrahedron. After the solid−solid transformation reaction for 30 min, the local environment around Ga is rapidly converted into tetrahedra from octahedra, which is in good agreement with the XRD observation on the collapse of interlayer $Ga_{13}$ polycations. The final reaction product corresponding to sodalite phase (f) shows a distinct peak at 10 373 eV, indicating that all the Ga species are stabilized in the tetrahedral site only. The second peak in the postedge region is attributed to a multiple scattering of photoelectrons by neighboring atoms. These results show that the Ga atoms in interlayer $Ga_{13}$ polycations are changed into the tetrahedral species, giving rise to the formation of sodalite framework.

**Ga K-Edge EXAFS.** Figure 5 shows the $k^3$-weighted Ga K-edge EXAFS spectra of the GIC and the reaction products. Clear changes can be seen around $k$ = 4, 6, and 8 Å$^{-1}$ where the EXAFS wave shifts to high $k$ value as the reaction time increases. Such changes in the EXAFS spectra become clearer as revealed in the radial distribution functions (RDFs) in Figure 6, which are obtained by Fourier transforms in the 2.65∼13.65 Å$^{-1}$ regions. Peaks in the range of 1∼2 Å are assigned to the

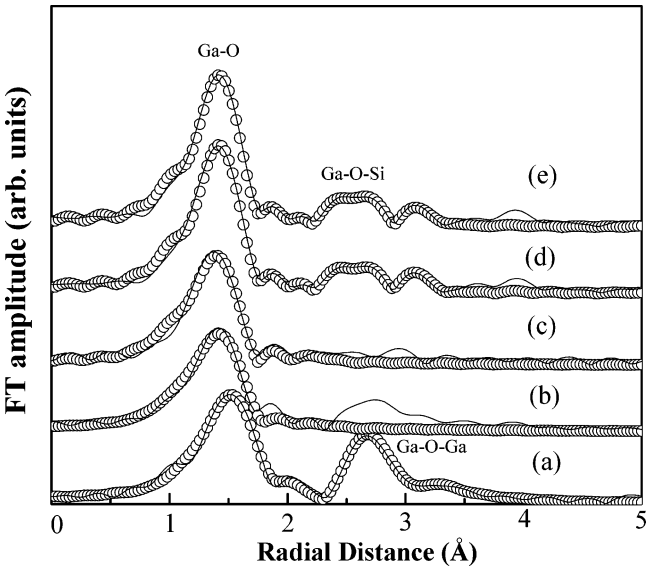


**Figure 6.** Fourier transformed Ga K-edge EXAFS spectra for (a) GIC, (b) after preparing the solid gel mixture of GIC and NaOH and the solid−solid transformation reaction for (c) 30 min, (d) 80 min, and (e) 240 min. The solid lines and empty circles represent the experimental and fitted data, respectively.

adjacent oxygen atoms around Ga, while those in 2∼3 Å result from backscattering of the second-neighboring metal atoms (Ga or Si). The spectra of $Ga_{13}$-intercalated clay and the resultant products were fitted by taking into account the crystallographic structure of $Ga_{13}$ polycation and sodalite, respectively.[10,15−16] There is a good correlation between experimental and calculated spectra (Figure 6). Unfortunately, the second coordination shell for the solid gel mixture of GIC (b) could not be fitted properly, which is due to the fact that the environment around the Ga atoms beyond the second shell is quite disordered. The curve fitting results are summarized in Table 1. As can be seen in Figure 6, the peaks of the FT spectra could be assigned to Ga−O, Ga···Ga(Si), and Ga···Na ($H_2O$) coordination, respectively.

For the first coordination shell (Ga−O) of the GIC, an excellent fit could be obtained by two subshells of oxygen neighbors at 1.93 ± 0.01 and 2.00 ± 0.01 Å, which is in agreement with the literature.[9,17] The relative Ga−O peak

**TABLE 1: Fitting Results for Ga K-edge EXAFS Spectra of GIC and the Reaction Products Obtained at the Various Stages of the Solid−Solid Transformation at 80 °C under an Ambient Atmosphere**

| | bond | distance (Å) | coord. no. (CN) | Debye-Waller factor($\sigma^2$) | $\Delta E_0$ |
|---|---|---|---|---|---|
| GIC | Ga−O | 1.93 | 3.0 | 0.0081 | 5.44 |
| | Ga−O | 2.00 | 2.9 | 0.0107 | 7.28 |
| | Ga···Ga | 3.00 | 4.0 | 0.0113 | −1.26 |
| | Ga···Ga | 3.40 | 7.0 | 0.0182 | −4.83 |
| solid gel mixture | Ga−O | 1.87 | 5.1 | 0.0094 | 0.25 |
| 30 min | Ga−O | 1.84 | 4.0 | 0.0058 | −0.90 |
| 80 min. | Ga−O | 1.83 | 4.0 | 0.0039 | 1.99 |
| | Ga···Si | 3.04 | 1.5 | 0.0025 | −3.41 |
| | Ga···Si | 3.18 | 2.5 | 0.0026 | −1.34 |
| 240 min (sodalite) | Ga−O | 1.83 | 4.0 | 0.0035 | 2.03 |
| | Ga···Si | 3.04 | 1.5 | 0.0019 | −3.64 |
| | Ga···Si | 3.18 | 2.5 | 0.0024 | −1.59 |

intensity in the GIC spectrum is lower than that in reaction products, despite an increase of oxygen coordination number of Ga, indicating that the structural disorder around Ga atoms in GIC is larger than that of the reaction products. This is also supported by an increase of Debye−Waller factor ($\sigma^2$), as summarized in Table 1. The Ga environments are rapidly transformed into tetrahedral environments with a Ga−O distance of 1.84 Å along with the expense of a second Ga···Ga shell at the beginning of the reaction, as revealed in the XRD and XANES spectra. After the reaction has proceeded for 30 min (c), the second coordination shell (Ga−O−Ga) disappears, suggesting that the Ga atoms may have various higher-shell coordination environments such as Ga−O−Si, Ga−O−Ga, and Ga···Na or Ga···$H_2O$. Consequently, the peak intensity due to multiple scattering becomes smaller because several types of disorder reduce the backscattering amplitudes.

After the formation of sodalite by the solid−solid transformation, the Ga−O bond distance decreases from 1.93 and 2.00 to 1.83 Å, which is well consistent with that of gallosilicate sodalite.[14,18] For the second-neighboring environment, two types of species (Ga···Si) could be obtained from fitting results. According to a Ga−O−Ga(Al) avoidance similar to Loewenstein's rule for aluminosilicate zeolite,[19] the sodalite framework could be formed by corner-sharing $[SiO_4]^{4-}$ tetrahedra linked with both $[AlO_4]^{5-}$ and $[GaO_4]^{5-}$ because the aluminum atoms are present along with gallium in starting materials. Therefore, the framework of resultant sodalite contains the Ga−O−Si and Al−O−Si bridges, thereby allowing two types of second-neighboring environments (Ga···Si···Ga(Al)) around Ga in sodalite structure. Consequently, two Ga−O−Si species with different bond angles result in the difference of Ga···Si bond distances. This provides also clear evidence that Ga atoms are incorporated into the sodalite framework through solid−solid transformation.

One important aspect in the EXAFS results is that the second Ga···Si shell corresponding to the Ga−O−Si species in the sodalite framework appears without any noticeable change in Ga−O bond distance. These suggest that $Ga(OH)_4^-$ ions generated from $Ga_{13}$ polycation react with corner-sharing $SiO_4$ in a silicate layer, giving rise to the Ga−O−Si gallosilicate network, in which the formation of gallosilicates and subsequent delocalized nucleation within the very limited dimension involves at least a solution-mediated reaction. Therefore, these results clearly explain that crystallization commences along with the formation of a gallosilicate network in a delocalized region and crystallization takes place over an entire clay lattice simultaneously. As a result, the solid−solid transformation mechanism could be understood as the limited crystal growth through the rearrangement of delocalized nuclei formed by at least a solution-mediated process as our previous reports indicate.[5] In addition, the crystalline sodalite phase from $Al_2O_3$ pillared clay was formed even within 10 min at 80 °C. However, the GIC exhibits a relatively slow transformation rate, which is ascribed to the polarization effect between Ga and Al.[7,20] It is considered that the crystallization rate depends on the nature of the trivalent metal cations and on their ability to react with silicate. These results reveal that the trivalent cations, such as Al and Ga, play an important role in the formation of zeolite framework through the solid−solid transformation.

## Conclusion

The gallosilicate sodalite was successfully synthesized by solid−solid transformation from the GIC, in which the intercalated Ga species play an important role in the formation of sodalite framework. At the initial stage of solid−solid transformation, Ga atoms formed by the collapse of $Ga_{13}$-polycation are gradually incorporated into the tetrahedral $SiO_4$ network like a solution-mediated process, which facilitates the rapid transformation into sodalite nuclei without drastic mass transport at gallium, aluminum, or silicon. That is, the solid−solid transformation mechanism involves at least a solution-mediated process in the minimum reaction of the gallium, silicon, and aluminum atoms. The crystal growth takes place mainly via the rearrangement of delocalized nuclei. In addition, it is found through the elucidation of the formation mechanism of Ga−O−Si species that the solid−solid transformation is strongly influenced by the trivalent cations, which are rapidly changed in the environment, followed by reacting with the silicate network of clay.

**Acknowledgment.** This research was supported by the Korean Research Foundation Grant (KRF-2004-041-C00187) and National R&D project for Nano Science and Technology. The authors are grateful for the financial support to participate in the international conference by the Science and Technology Amicable Research (STAR) Program of the Ministry of Science and Technology.

## References and Notes

(1) (a) Cundy, C. S.; Cox, P. A. *Chem. Rev.* **2003**, *103*, 663. (b) Lee, J. S.; Lee, Y. J.; Tae, E. L.; Park, Y. S.; Yoon, K. B. *Science* **2003**, *301*, 818. (c) Mintova, S.; Olson, N. H.; Valtchev, V.; Bein, T. *Science* **1999**, *283*, 950. (d) Wang, H.; Holmberg, B. A.; Yushan, Y. *J. Am. Chem. Soc.* **2003**, *125*, 9928.

(2) (a) Walton, R. I.; O'Hare, D. *J. Phys. Chem. B* **2001**, *105*, 91. (b) Walton, R. I.; Millange, F.; O'Hare, D.; Davies, A. T.; Sankar, G.; Catlow, C. R. A. *J. Phys. Chem. B* **2001**, *105*, 83. (c) Davis, M. E.; Lobo, R. F. *Chem. Mater.* **1992**, *4*, 756. (d) Dutta, P. K.; Shieh, D. C. *J. Phys. Chem.* **1986**, *90*, 2331.

(3) (a) Serrano, D. P.; Van Grieken, R. *J. Mater. Chem.* **2001**, *11*, 2391. (b) Serrano, D. P.; Van Crieken, R.; Sanchez, P.; Sanz, R.; Rodriguez, L. *Microporous Mesoporous Mater.* **2001**, *46*, 35. (c) Xu, W.; Dong, J.; Li, J.; Li, J.; Wu, F. *J. Chem. Soc., Chem. Commun.* **1990**, 755.

(4) (a) Choi, C. L.; Park, M.; Lee, D. H.; Kim, J. E.; Park, B. Y.; Choi, J. *Environ. Sci. Technol.* **2001**, *35*, 2812. (b) Afanasiev, P. *Chem. Mater.* **2001**, *13*, 459.

(5) (a) Choy, J. H.; Lee, S. R.; Han, Y. S.; Park, M.; Park, G. S. *Chem. Commun.* **2003**, 1922. (b) Lee, S. R.; Han, Y. S.; Park, M.; Park, G. S.; Choy, J. H. *Chem. Mater.* **2003**, *15*, 4842. (c) Lee, S. R.; Han, Y. S.; Choy, J. H. *Solid State Ionics* **2002**, *151*, 343.

(6) (a) van Bokhoven, J. A.; van der Eerden, A. M. J.; Koningsberger, D. C. *J. Am. Chem. Soc.* **2003**, *125*, 7435. (b) Fröba, M.; Wang, J.; Behrens, P.; Sieger, P.; Rowen, M.; Tanaka, T.; Rek, Z.; Felsche, J. *Physica B* **1995**, *208−209*, 65.

(7) (a) Fricke, R.; Kosslick, H.; Lischke, G.; Richter, M. *Chem. Rev.* **2000**, *100*, 2303. (b) Axon, S. A.; Huddersman, K.; Klinowski, J. *Chem. Phys. Lett.* **1990**, *172*, 398. (c) Cho, H. H.; Kim, S. H.; Kim, Y. G.; Kim, Y. C.; Koller, H.; Camblor, M. A.; Hong, S. B. *Chem. Mater.* **2000**, *12*, 2229.

(8) (a) Choy, J. H.; Hwang, S. J.; Park, N. G. *J. Am. Chem. Soc.* **1997**, *119*, 1624. (b) Hwang, S. J.; Choy, J. H. *J. Phys. Chem. B* **2003**, *107*, 5791.

(9) Montargès, E.; Michot, L. J.; Ildefonse, P. *Microporous Mesoporous Mater.* **1999**, *28*, 83.

(10) Bradley, S. M.; Kydd, R. A.; Yamdagni, R. *J. Chem. Soc., Dalton Trans.* **1990**, 2653.

(11) (a) Wilson, M. J. *Clay Mineralogy: Spectroscopic and Chemical Determinative Methods*; Chapman & Hall: London, UK, 1994. (b) Madejová, J. *Vib. Spectrosc.* **2003**, *31*, 1.

(12) (a) Herreros, B.; Klinowski, J. *J. Chem. Soc., Faraday Trans.* **1995**, *91*, 1147. (b) Bibby, D. M.; Dale, M. P. *Nature* **1985**, *317*, 157.

(13) Godber, J.; Ozin, G. A. *J. Phys. Chem.* **1988**, *92*, 4980.

(14) (a) Nishi, K.; Shimizu, K. I.; Takmatsu, M.; Yoshida, H.; Satsuma, A.; Tanaka, T.; Yoshida, S.; Hattori, T. *J. Phys. Chem. B* **1998**, *102*, 10190. (b) Behrens, P.; Kosslick, H.; Tusan, V. A.; Fröba, M.; Neissendorfer, F. *Microporous Mater.* **1995**, *3*, 433.

(15) (a) Johansson, G. *Acta Chem. Scand.* **1962**, *16*, 403. (b) Bradley, S. M.; Kydd, R. A.; Yamdagni, R. *J. Chem. Soc., Dalton Trans.* **1990**, 413.

(16) (a) Hassan, I.; Grundy, H. D. *Acta Crystallogr.* **1984**, *B40*, 6. (b) Felsche, J.; Luger, S. *Thermochim. Acta* **1987**, *118*, 35.

(17) Michot, L. J.; Montargès-Pelletier, E.; Lartiges, B. S.; de la Caillerie, J. B. d'E.; Briois V. *J. Am. Chem. Soc.* **2000**, *122*, 6048.

(18) Behrens, P.; Felsche, J.; Niemann, W. *Catal. Today* **1991**, *8*, 479.

(19) Loewentein, W. *Am. Miner.* **1954**, *39*, 92.

(20) Huheey, J. E.; Keiter, E. A.; Keiter, R. L. *Inorganic Chemistry: Principle of Structure and Reactivity*, 4th ed; HarperCollins College Publishers: New York, 1993.